Spectroscopy and Such (Working Title)

By
Blaise Jonathan Thompson

A dissertation submitted in partial fulfillment of
the requirements for the degree of

Doctor of Philosophy
(Chemistry)

at the
UNIVERSITY OF WISCONSIN - MADISON
20xx

Date of final oral examination: xx/xx/xxxx
This dissertation is approved by the following members of the Final Oral Committee:
John C. Wright, Professor, Analytical Chemistry
x
x
x
x

Contents

List of Figures

List of Tables

Acknowledgments

Abstract

The explanatory stories that people find compelling are simple; are concrete rather than abstract; assign a larger role to talent, stupidity and intentions than to luck; and focus on a few striking events that happened rather than on the countless events that failed to happen.

The ultimate test of an explanation is whether it would have made the event predictable in advance.

Paradoxically, it is easier to construct a coherent story when you know little, when there are fewer pieces to fit into the puzzle. Our comforting conviction that the world makes sense rests on a secure foundation: our almost unlimited ability to ignore our ignorance.

– Daniel Kahneman [1]

Chapter 1

Introduction

1.1 Coherent Multidimensional Spectroscopy

CMDS, coherent multidimensional spectroscopy

1.2 The CMDS Instrument

From an instrumental perspective, MR-CMDS is a problem of calibration and coordination. Within the Wright Group, each of our two main instruments are composed of roughly ten actively moving component hardwares. Many of these components are purchased directly from vendors such as SpectraPhysics, National Instruments, Horiba, Thorlabs, and Newport. Others are created or heavily modified by graduate students. The Wright Group has always maintained custom acquisition software packages which control the complex, many-stepped dance that these components must perform to acquire MR-CMDS spectra.

1.3 Scientific Software

When I joined the Wright Group, I saw that acquisition software was a real barrier to experimental progress and flexibility. Graduate students had ideas for instrumental enhancements that were infeasible because of the challenge of incorporating the new components into the existing software ecosystem. At the same time, students were spending much of their time in lab repeatedly calibrating optical parametric amplifiers by hand, a process that sometimes took days. I chose to spend a significant portion of my graduate career focusing on solving these problems through software development. At first, I focused on improving the existing LabVIEW code. Eventually, I developed a vision for a deeply modular acquisition software that could not be practically created with LabVIEW. Using Python and Qt, I created a brand new acquisition software PyCMDS: built from the ground up to fundamentally solve historical challenges in the Group. PyCMDS offers a modular hardware model that can "re-configure" itself to flexibly control a variety of component hardware configurations. This has enabled graduate students to add and remove hardware whenever necessary, without worrying about a heavy additional programming burden. PyCMDS is now used to drive both MR-CMDS instruments in the Group, allowing for easy sharing of component hardware and lessening the total amount of software that the Group needs to maintain. Besides being more flexible, PyCMDS solves a number of other problems. It offers fully automated strategies for calibrating component hardwares, making calibration less arduous and more reproducible. It offers more fine-grained control of data acquisition and timing, enabling more complex algorithms to quickly acquire artifact-free results. In conjunction with other algorithmic and hardware improvements that I have made, PyCMDS has decreased acquisition times by up to two orders of magnitude. A companion software, WrightTools (which I also created), solves some of the processing and representation challenges of multidimensional data.

Part I

Background

Part II

Instrumental Development

Part III

Applications

Chapter 2

PEDOT:PSS

2.1 Introduction

Poly(3,4-ethylenedioxythiophene)-poly(styrenesulfonate) (PEDOT:PSS) is a transparent, electrically conductive (up to 4380 S cm^{-1} [2]) polymer. It has found widespread use as a flexible, cheap alternative to inorganic transparent electrodes such as indium tin oxide.

As a polymer, PEDOT:PSS implicitly contains a large amount of structural inhomogeneity. On top of this, PEDOT:PSS is a two component material, composed of PEDOT (low molecular weight, p-doped, highly conductive) and PSS (high molecular-weight, insulating, stabilizing). These two components segment into domains of conductive and non-conductive material, leading to even more structural inhomogeneity. Nonlinear spectroscopy may be able to shed light on the microscopic environment of electronic states within PEDOT:PSS.

2.2 Background

Complex microstructure:

1. PEDOT oligomers (6—18-mers)
2. these oligomers π-stack to form small nanocrystalites, 3 to 14 oligomers for pristine films to as many as 13—14 oligomers for more conductive solvent treated films
3. nanocrystallites then arrange into globular conductive particles in a pancakge-like shape
4. these particles themselves are then linked via PSS-rich domains and assembled into nanofibril geometry akin to a string of pearls
5. nanofibrils interweave to form thin films, with PSS capping layer at surface

Prior spectroscopy (absorption anisotropy, X-ray scattering, condutivity).

Broad in the infrared due to midgap states created during doping from charge-induced lattice relaxations. These electronic perturbations arise from injected holes producing a quinoidal distortion spread over 4-5 monomers of the CP aromatic backbone, collectively called a polaron. Energetically favorable to be spin-silent bipolaron.

2.3 Methods

PEDOT:PSS (Orgacon Dry, Sigma Aldrich) was dropcast onto a glass microscope slide at 1 mg/mL at a tilt to ensure homogeneous film formation. The sample was heated at 100 °C for ∼15 min to evaporate water.

An ultrafast oscillator (Spectra-Physics Tsunami) was used to prepare ∼35 fs seed pulses. These were amplified (Spectra-Physics Spitfire Pro XP, 1 kHz), split, and converted into 1300 nm 40 fs pulses using two separate optical parametric amplifiers (Light Conversion TOPAS-C): "OPA1" and "OPA2". Pulses from OPA2 were split again, for a total of three excitation pulses: ω_1, ω_2 and $\omega_{2'}$. These were passed through motorized (Newport MFA-CC) retroreflectors to control their relative arrival time ("delay") at the sample: $\tau_{21} = \tau_2 - \tau_1$ and $\tau_{22'} = \tau_2 - \tau_{2'}$. The three excitation pulses were focused into the sample in a 1° right-angle isoceles triange, as in the BOXCARS configuration. [3] Each excitation beam was 67 nJ focused into a 375 μm symmetric Gaussian mode for an intensity of 67 μJ/cm^2. A new beam, emitted coherently from the sample, was isolated with apertures and passed into a monochromator (HORIBA

Jobin Yvon MicroHR, 140 mm focal length) with a visible grating (500 nm blaze 300 groves per mm). The monochromator was set to pass all colors (0 nm, 250 μm slits) to keep the measurement impulsive. Signal was detected using an InSb photodiode (Teledyne Judson J10D-M204-R01M-3C-SP28). Four wave mixing was isolated from excitation scatter using dual chopping and digital signal processing.

2.4 Transmittance and reflectance

?? shows the transmission, reflectance, and extinction spectrum of the thin film used in this work.

2.5 Three-pulse echo spectroscopy

Two dimensional $\tau_{21}, \tau_{22'}$ scans were taken for two phase matching configurations: (1) $k_{\text{out}} = k_1 - k_2 + k_{2'}$ (3PE) and (2) $k_{\text{out}} = k_1 + k_2 - k_{2'}$ (3PE*). The rephasing and nonrephasing pathways exchange their time dependance between these two configurations. Comparing both pathways, rephasing-induced peak shifts can be extracted as in 3PE. [CITE] All data was modeled using numerical integration of the Liouville-von Numann equation.

Continuously variable ND filters (THORLABS NDC-100C-4M, THORLABS NDL-10C-4) were used to ensure that all three excitation pulse powers were equal within measurement error.

2.6 Frequency-domain transient grating spectroscopy

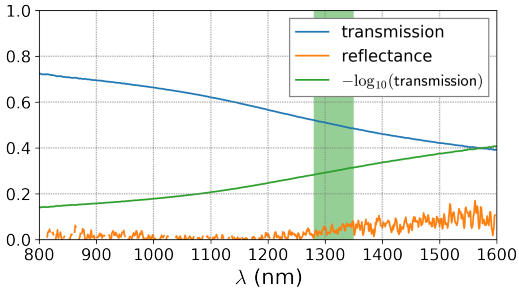

Figure 2.1: Thin film spectra. Transmission, reflectance, and extinction spectrum of the thin film used in this work. Extinction is $\log_{10}$(transmission).

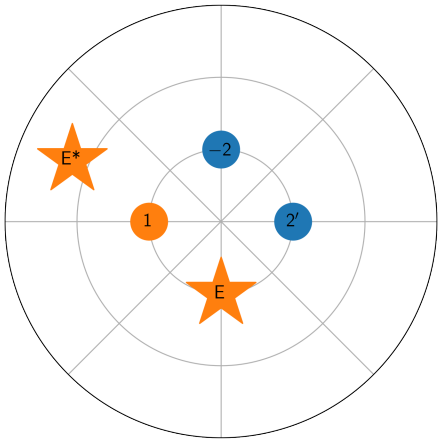

Figure 2.2: Phase matching mask used in this experiment. Each successive ring subtends 1 degree, such that the excitation pulses are each angled one degree relative to the mask center. The two stars mark the two output poyntings detected in this work.

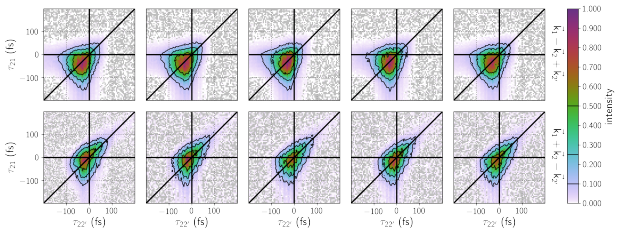

Figure 2.3: CAPTION TODO

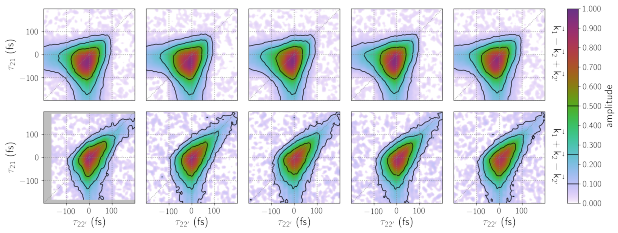

Figure 2.4: CAPTION TODO

Figure 2.5: CAPTION TODO

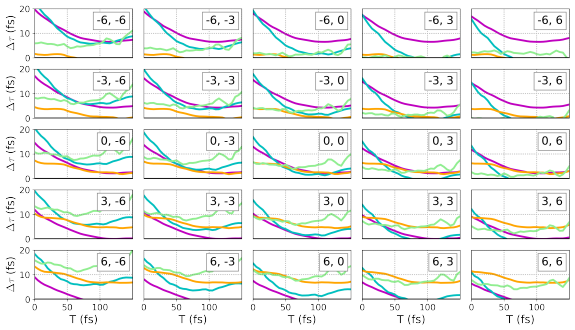

Figure 2.6: CAPTION TODO

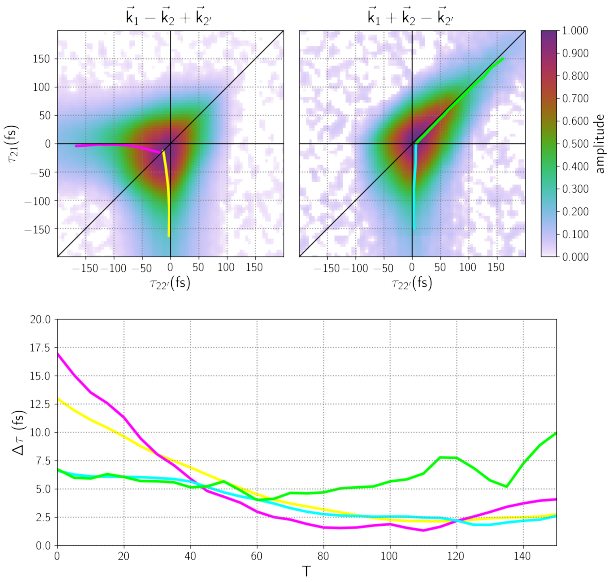

Figure 2.7: CAPTION TODO

Part IV

Appendix

Bibliography

[1] Daniel Kahneman. *Thinking, Fast and Slow*. Farrar, Straus and Giroux, 2013. ISBN: 9780374533557.

[2] Nara Kim, Seyoung Kee, Seoung Ho Lee, Byoung Hoon Lee, Yung Ho Kahng, Yong-Ryun Jo, Bong-Joong Kim, and Kwanghee Lee. "Highly Conductive PEDOT:PSS Nanofibrils Induced by Solution-Processed Crystallization". In: *Advanced Materials* 26.14 (Dec. 2013), pp. 2268–2272. DOI: 10.1002/adma.201304611.

[3] Alan C. Eckbreth. "BOXCARS: Crossed-beam phase-matched CARS generation in gases". In: *Applied Physics Letters* 32.7 (Apr. 1978), pp. 421–423. DOI: 10.1063/1.90070.